Beam Splitting with a Luminescent Solar Concentrator in a Hybrid Photovoltaic/Thermal Collector

Maja Gajic[1], David Rodriguez-Sanchez[1] and Gary Rosengarten[1]

[1] RMIT University, School of Engineering, Melbourne (Australia)

Abstract

This work investigates the combination of two non-imaging types of concentrating solar technologies: the luminescent solar concentrator, that generates electricity via photovoltaic cells and the compound parabolic concentrator, used normally with a thermal receiver. The luminescent solar concentrator in this new application is used as a cover for the solar thermal collector (the CPC) whilst at the same time concentrating a specific wavelength band of light to its edges where solar PV cells convert photons to electricity. Absorption of a part of the solar spectrum occurs in the LSC, whilst the rest of the solar spectrum can be captured as thermal energy in the CPC, essentially forming a new type of spectral splitting hybrid solar collector that can produce electricity and medium temperature heat. A small prototype hybrid CPC and LSC collector was tested in the lab using a solar simulator. This proof of concept device compared a high transmission and low transmission LSC and demonstrated the experimental basis of the new type of PV-T collector. An outdoors flow experiment was undertaken, measuring instantaneous thermal efficiency and electrical output.

Keywords: solar photovoltaic, solar thermal, hybrid

1. Introduction

The sun is the world's most abundant energy source and means of harvesting it include photovoltaic cells to create electricity and solar thermal collectors to generate heat. Low temperature heat can be used for domestic applications where in urban environments available space is often limited. By combining solar thermal and photovoltaics in one system, roof space can be saved and potentially efficiency can be increased. Photovoltaic technologies can only convert photons with energies above their bandgap to electricity, with the remainder of the solar spectrum wastefully generating heat. In a hybrid configuration that heat is not wasted but collected instead.

This work combines for the first time two types of non-imaging solar concentrators, the luminescent solar concentrator (LSC) and the compound parabolic solar thermal collector in a hybrid configuration as shown in Fig. 1. The LSC cover acts as a beam splitter of solar radiation. The absorption and emission spectra of the fluorescent molecules within the LSC device select a part of the spectrum, where ideally it is totally internally reflected to the solar PV cells attached to the edges of the LSC. The rest of the solar spectrum is transmitted through the LSC cover to the solar thermal collector.

There are many potential applications for such a technology depending on what the desired outcome is. The CPC solar thermal collector can be designed for domestic applications requiring low temperature heat or for commercial applications where medium temperature heat is required (up to approximately 200 °C). Currently the LSC can generate modest amounts of electricity that could potentially power peripheral devices or sensors. This is due to the low power conversion efficiencies of the device, with the world record device achieving 7.1 % with expensive gallium arsenide PV cells (Slooff et al., 2008).

There is of course a trade-off between electricity generated and thermal energy collected and one or the other could be prioritised depending on loads and needs. The potential applications for hybrid photovoltaic and thermal (PV-T) collectors are more numerous in urban environments where roof space is often limited (Ramos et al., 2017). By making better use of the solar source, PV-T collectors can save on space and improve energy collection efficiency.

doi:10.18086/swc.2017.20.02 Available at http://proceedings.ises.org

2. Hybrid CPC and LSC Collector

2.1 Luminescent solar concentrator

Luminescent solar concentrators consist of a fluorescent material embedded in a waveguide such as poly methyl methacrylate (PMMA). Photons that fall within the absorption spectrum of the fluorescent material can be absorbed and then isotropically emitted at a longer wavelength. Ideally these re-emitted photons are propagated to the edge of the waveguide via total internal reflection (Debije and Verbunt, 2012). Solar PV cells (or other absorbers) can then be attached to the edges of the device to convert photons to electricity. An important benefit of LSCs is that they can concentrate both diffuse and beam radiation (Smestad et al., 1990) and they have a wide acceptance angle, which allows them to function without tracking. The acceptance angle is defined as the maximum angular deviation of a ray with respect to the normal to the aperture plane, which allows the ray to be intercepted by the receiver. Additionally, the fluorescent dye can be chosen to emit photons that the solar PV cells can convert with higher efficiency. Conventionally their use has been envisaged to be in the urban environment to reduce the environmental impact of buildings (Gajic et al., 2017; Kanellis et al., 2017).

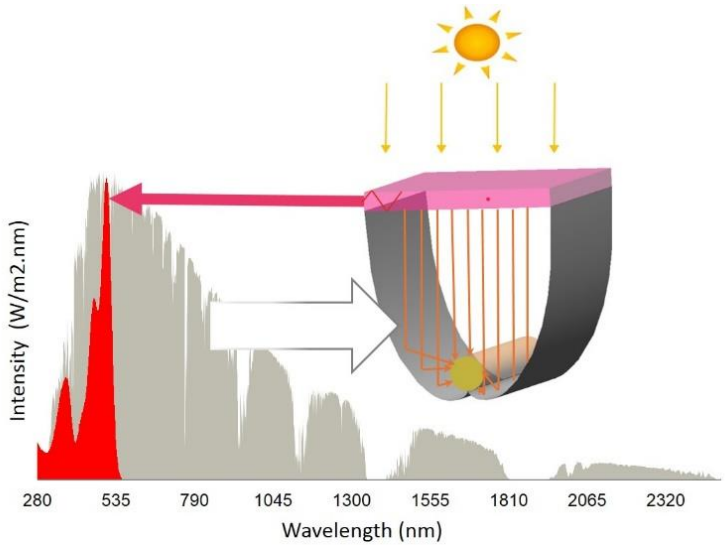

Fig. 1: Schematic of LSC and CPC hybrid collector overlaid with solar AM 1.5 spectrum (grey) and Lumogen Red 3505 fluorescent dye absorption spectrum (red)

2.2 LSC design and fabrication

For the small-scale prototype hybrid CPC and LSC, two LSCs were fabricated from commercially available fluorescent sheets as shown in Fig. 2. A pink sheet, commercially manufactured by Evonik ("Evonik Industries," 2017) and a red sheet named Mars Red 4t56 available from online retailers. The properties of the LSCs are summarised in Table 1. Since these fluorescent sheets were commercially procured, it was not possible to determine the exact concentration of fluorescent dye or even confirm the fluorescent material. The pink sheet is assumed to contain the dye Lumogen Red 305, estimated from spectroscopic properties. The solar AM 1.5 averaged absorption was measured for the pink sheet to be 8.6 % and red sheet to be 32.8 %. The high transparency of the pink sheet is useful for collecting most of the energy as heat in the solar thermal collector while the higher absorbing red sheet transmits more energy to the PV cells. The absorption spectra of the two LSCs and the AM 1.5 spectrum is shown in Fig. 3. The figure shows how that the red sheet absorbs much more of the visible spectrum than the pink sheet, which will enhance transmission to the PV cells. The fluorescent sheets were cut to size and the edges were optically polished with very fine sand paper and polishing oil. Sunpower high efficiency back contact PV cells were diced and cut to fit the edge of the LSC. These cells are very well suited to LSC applications as they have all the wiring on the back. The thickness of the cells is 3 mm and for the prototype LSCs, cells of length 9.5 cm and 5 cm were fabricated. The pink and red LSCs have the 9.5 cm cells placed along the 10 cm edge of the LSC and along the 15 cm length both 9.5 cm and 5 cm cells were attached. Each had attached wiring that was connected in parallel externally.

Tab. 1: LSC prototype specifications

LSC specifications	Value
Size	10 x 15 x 0.3 cm
Geometric concentration ratio	15
Optical coupling	Silicone Elastosil Solar 2202
Red fluorescent material	Unknown
Pink fluorescent material	Lumogen Red 305
LSC waveguide	Perspex
Fluorescent dye concentration	Unknown
Solar PV cells	Sunpower PV cell cut to 3 mm thick, edge coupled

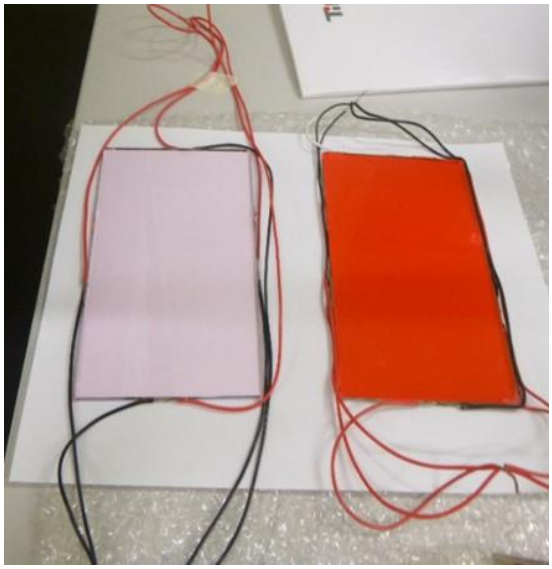

Fig. 2: Pink LSC (left) and red LSC (right)

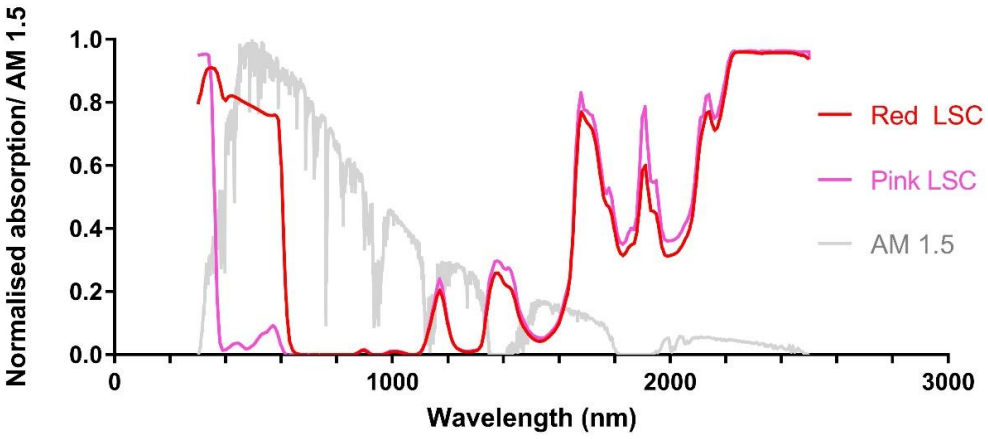

Fig. 3: AM 1.5 solar spectrum (grey) overlaid with the pink LSC absorption spectrum and red LSC absorption

2.3 Compound parabolic concentrator

The compound parabolic concentrator was developed by Roland Winston when he was investigating means of efficiently detecting Cherenkov radiation (Hinterberger, 1966). The discovery of the CPC led to the development of the field of non-imaging optics, whose designs approach and even realise the maximum concentration allowable for a given acceptance angle, due to removing the need for point to point mapping required by conventional optics (Rabl and Winston, 1976; Winston, 1970; Winston et al., 2009; Winston and Welford, 1978).

Ideally, the CPC concentrates all rays that fall within its acceptance half angle, Θ_A. The acceptance angle will determine the hours of light that can be collected as CPC designs are almost always non-tracking. The concentration ratio *C* of a two-dimensional CPC is determined by the ratio of the aperture area to the area of the receiver and quantifies the increase of solar flux on the receiver. *C* is inversely related to the acceptance angle and this means we can achieve higher concentration ratios, but at the expense of hours of sunlight that can be concentrated. A two-dimensional CPC can be considered as trough like and this shape is ideal for thermal applications where a cylindrical receiver such as an evacuated tube can be placed along the focal length of the collector (Herrick, 1982; Karwa et al., 2015). A cross sectional view is shown in Fig. 4. An involute shape CPC with an entrance aperture, d_1, and receiver radius, *r*, has a concentration ratio as shown in eq. 1. Θ_A is the acceptance half angle and ideally all incident rays at and below this angle will be transmitted to the receiver.

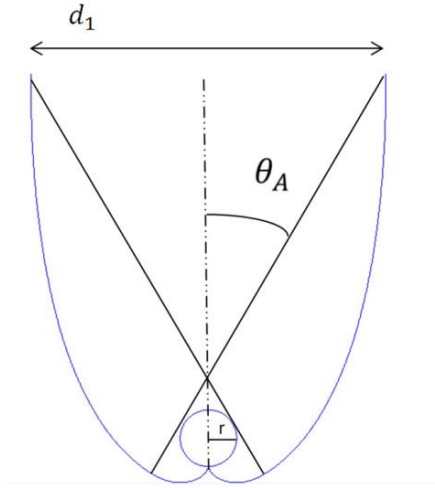

Fig. 4: Involute shaped compound parabolic concentrator

$$\text{Concentration ratio} = \frac{1}{\sin(\theta_A)} = \frac{d_1}{2\pi r} \qquad \text{(eq. 1)}$$

There is a large potential for solar technologies to meet industrial process heat needs, where medium temperatures are required (90 - 250 ˚C). CPCs offer a simple robust solution that has the potential to meet these needs. It has also been shown that CPCs can perform better than other solar collectors over a wide range of temperatures and without tracking (Brunold et al., 1994; Carvalho et al., 1995; Gallagher et al., 1993; Gu et al., 2014). As CPCs can reach the maximum allowed concentration for a given acceptance angle they are the best choice for a proof of concept collector that utilises a cover made up of a luminescent solar concentrator.

2.4 Compound parabolic concentrator for proof of concept hybrid collector

A small proof of concept prototype CPC and LSC hybrid was developed in this work. The CPC is designed with an aperture area of 15 cm and an absorber of radius 0.87 cm, giving a concentration ratio on the absorber of 2.74. An extruded profile of length 10 cm was generated and using CAD software, a profile was created as shown in Fig. 5 (right). The height was truncated by 70 % to save on material costs and to allow for a thinner collector

profile. The profile was then 3D printed with ABS polymer, and coated with highly reflective sputtered aluminium. The properties of the CPC are summarised in Table. 2. The involute compound parabolic shape was designed to be combined with a cylindrical receiver made up of an absorber within an evacuated tube and a 3 mm clearance gap between absorber and glass envelope. The evacuated receiver was supplied by commercial suppliers. However, the datasheet of the selective surface was not provided. The hybrid prototype under test conditions is shown in Fig. 5 (left).

Tab.2: CPC specifications and values

CPC specifications	Value
Radius absorber	0.87 cm
Gap between absorber and glass	3 mm
Aperture	15 cm
Concentration ratio	2.74
Acceptance angle	21.4 ˚
Mirror reflectance	AM 1.5 averaged 91 %
Truncation of height	70 %
Cost to 3D manufacture	$ 200 (material cost only)

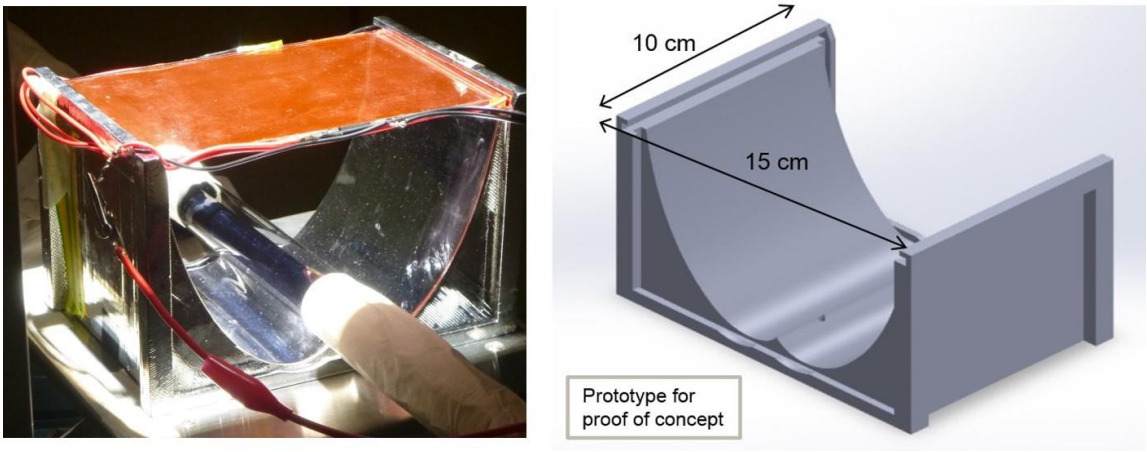

Fig. 5: Prototype hybrid under indoor test conditions (left), image of 3D printed prototype CPC (right)

4.2 Experimental setup

Indoor performance testing of the hybrid collector was analysed under a triple-A rated solar simulator. A 1000 W/m^2 radiation flux at the aperture plane of the CPC was set up using a calibrated pyranometer. To measure electrical performance of the LSC cover, I-V curves were taken with a Keithley 2400 source measuring unit. The indoor experimental set up is shown below in Fig. 6. The experiment compared both the pink and red LSC covers. I-V curves were measured under three different conditions shown below.

- LSC only (without the CPC) placed onto an absorbing material (TiNOX). This is necessary to stop reflected photons passing back into the LSC.
- LSC coupled with the CPC collector at the start of illumination (cold).
- LSC coupled with the CPC collector and after three hours of illumination (after 3 hours).

Thermal performance was characterised by measuring the stagnation temperature of various configurations of the device. Performance testing of solar collectors describes stagnation temperature as maximum achievable collector temperature. This occurs at zero flow conditions where the heat input is equal to the heat loss. The collector is illuminated at a constant radiation until this maximum temperature is reached, providing a useful comparison of the different configurations.

The thermal receiver used in the experiment is shown in Fig. 7. The 10 cm length required was left bare while the remainder of the tube was wrapped in foil and the ends were insulated. The tube is comprised of a selective surface absorber in an evacuated tube. To measure the stagnation temperature three k-type thermocouples were placed in the tube - one at the far end, one in the middle in the active area and one at the near end of the entrance.

A data logger is used to measure the temperature and the hybrid configuration was left to stagnate under the solar simulator for up to 3 or more hours, with at least 5 measurements made of each configuration.

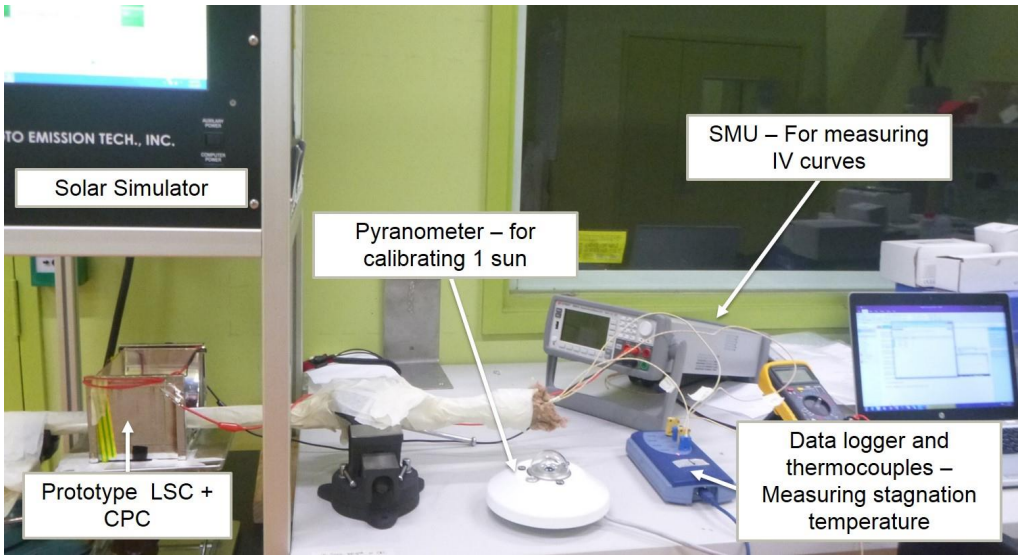

Fig. 6: Indoor experimental test setup

Fig. 7: Evacuated thermal receiver used in the stagnation tests

4.3 Results

The stagnation temperature test results on various configurations of the hybrid CPC and LSC are shown in Fig. 8. The stagnation temperatures reached for the different configurations (ambient subtracted) were: 208 ˚C for the CPC without an LSC cover, 192 ˚C for the CPC with the pink LSC cover, 150 ˚C for the CPC with the red LSC cover and 77 ˚C for the tube on its own under one sun illumination. This value is representative of the poor quality of these tubes we received from the manufacturer, an evacuated tube with a proper vacuum and a good selective surface should be able to stagnate at over 200 ˚C without concentration.

Pink and red LSC I-V curves were measured twice during the stagnation experiment; at the beginning of the experiment, and after three hours of continuous illumination under the solar simulator. The performance of both LSCs decreased after three hours, the pink LSC short circuit current reduced by 40 % and the red LSC short circuit current reduced by 16 % (results are summarised in Table 3). This is an interesting result considering LSCs are claimed to decouple the heat generating area, since it's the LSC that receives light and heats up and is thought not to transmit much heat to the solar PV cells around the edge. It remains unclear however if it is the PV cell around the edge of the device that is heating up, if the performance of the polymer itself is degrading or even if the behaviour of the fluorescent material changes with temperature. When the temperature of a polymer such as PMMA is increased its refractive index changes due to a change in its thermo-optic coefficient (Zhang et al., 2006). This behaviour has received little attention in LSC literature. An analysis of thermal performance of LSCs was completed by (Rajkumar et al., 2015), who studied the temperature of LSCs under illumination. The authors found the surface of the LSC reached a temperature of 50 ˚C after one hour and the edge mounted PV cells remained 10 ˚C cooler (the ambient temperature recorded in their lab was 21.5 ˚C and under the solar simulator was 34.5 ˚C). All these effects come into play as well as ambient temperature and presence of heat transfer due to convection (higher convective heat transfer coefficients outside than inside the lab).

Measurements were also taken by placing the LSC only, on a highly absorbent “black” material TiNOX that does not reflect any photons back into the LSC. The I-V curves under the various conditions are summarised in Fig. 9. It can be seen that simply placing the LSC on the CPC improves performance due to reflected photons from within the collector getting a chance to be captured by the LSC, that is the performance of the LSCs improves compared with simply measuring on a black absorber TiNOX. The reason for this is that some isotropically emitted photons from within the LSC are emitted into the CPC at angles that do not result in them being transmitted to the receiver and hence reflect back into the LSC. This is an interesting result showing LSCs perform better in this new application than on their own.

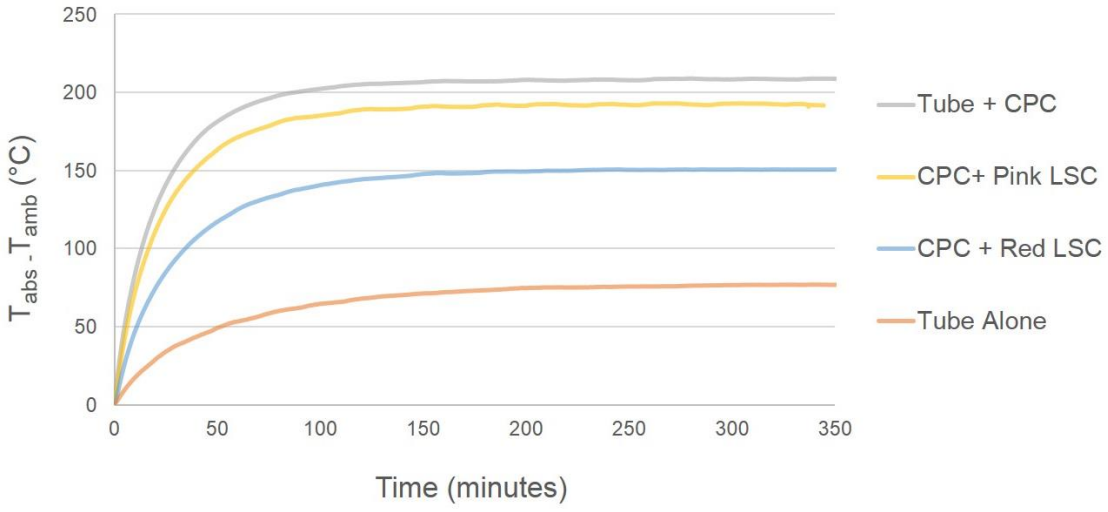

Fig. 8: Results of stagnation temperature test of hybrid CPC and LSC collector

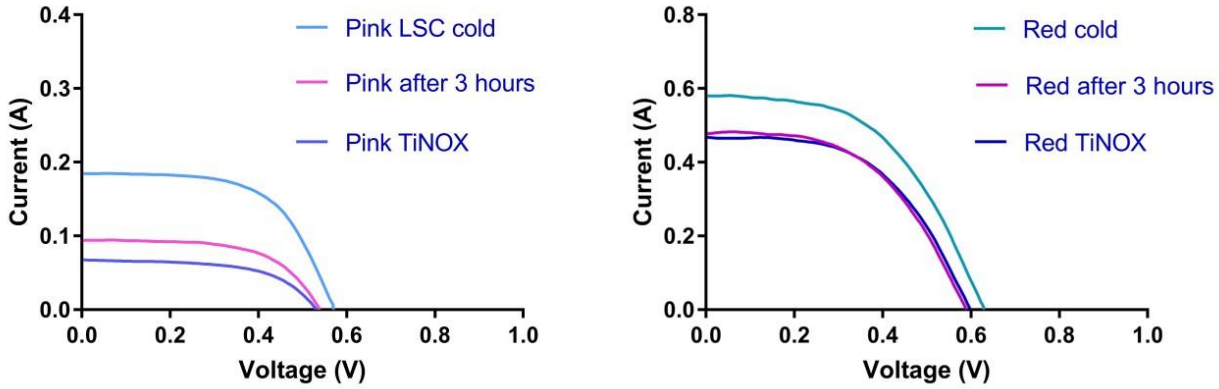

Fig. 1: I-V curves under different configurations of the hybrid prototype with the pink LSC (left) cover and red LSC cover (right)

Tab. 3: Summary of results

Hybrid prototype configuration	Short circuit current of LSC	Power conversion efficiency of LSC	Stagnation temperature (T_{abs}-T_{amb}) ˚C
Red LSC on CPC After 3 hours	485 mA	0.98 %	150 ˚C
Red LSC on CPC	578 mA	1.3 %	
Red LSC on TiNOX	473 mA	0.99 %	
Pink LSC on CPC After 3 hours	111 mA	0.2 %	191 ˚C
Pink LSC on CPC	185 mA	0.43 %	
Pink LSC on TiNOX	68 mA	0.14 %	
Evacuated tube on its own			77 ˚C

3. Full Scale Roof Experiment

3.1 Introduction

In the previous section a small prototype hybrid CPC and LSC was shown to reach high stagnation temperatures even with the LSC cover that absorbs a small proportion of the solar spectrum. In this section we extend this work to investigate a full length, 1-meter long CPC. This full-length collector was connected to a solar test rig on a rooftop facility at RMIT University in Melbourne as shown in Fig. 10. The collector was mounted in the east-west direction on the test rig and connected to a high temperature fluid delivery system. The CPC was covered with LSCs and flow experiments were performed whilst I-V measurements were made of the LSCs that had been wired together. This work demonstrates the benefits of using this system as a decoupled photovoltaic and thermal collector capable of delivering medium temperature heat and electricity.

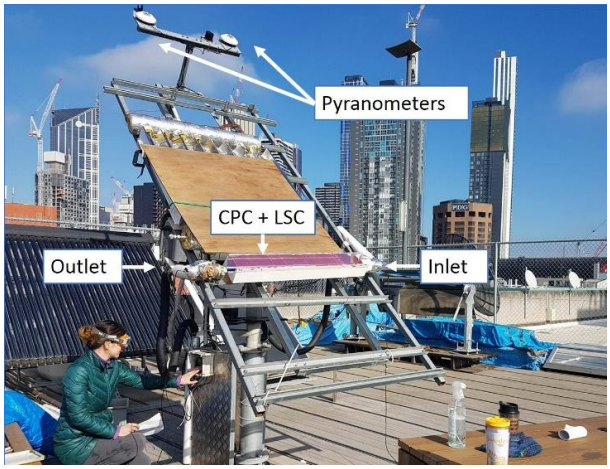

Fig. 10: Experimental setup for full length CPC and LSC collector mounted on two axis tracker

3.2 LSC design

A large sheet of Evonik PLEXIGLASS Red 3C50 GT was cut into four modules to cover the 1 m length CPC collector. Four modules of 25 cm length x 12 cm width were fabricated to cover the CPC collector. The thickness of the sheet was 3 mm and the edges were all polished until they became optically smooth using sandpaper and polishing oil. Sunpower back contact PV cells were coupled with silicone gel along the top edge and bottom edge but not sandwiched in between modules as they would heat up too much and it would be difficult to seal the collector.

3.3 CPC design

A one-meter length CPC was fabricated out of timber in the workshop using a CNC router. The specifications of the CPC are slightly different to section 2 of this paper, the properties of the receiver remain the same but the aperture is reduced to 11 cm. The CPC was sanded smooth and then coated with high gloss polyurethane ready for the reflective foil to be laid down. The reflective film, purchased from an online retailer was found to have a solar weighted reflectivity of 90 %. The receiver consisted of an evacuated tube with a selective surface absorber purchased from commercial suppliers, a second batch with the same specifications as the tube used in the indoor experiments.

3.4 Experimental setup

The CPC and LSC hybrid collector was mounted east-west orientation onto a test rig that also performs two-dimensional solar tracking. Tracking was used to keep the collector normal to the sun for performance measurements, to minimise as much as possible non-normal incidence angle effects. This is a standard method for testing solar collectors as found in the AS/NZS 2535.1:1999 standards. The hybrid collector is connected to the closed loop fluid delivery system that is composed of a heater and cooling fan that can control the input temperature of the collector via a PID controller and thermocouple at the heater outlet (not shown in Figures). To determine the collector efficiency several measurements need to be made: the fluid temperature at the collector inlet, T_{in}, the fluid temperature at the collector outlet $T_{out,}$ mass flow rate, irradiance incident on the collector and collector area. In this way the useful energy absorbed in the fluid (Therminol 66) can be calculated as shown in eq. 2.

$$Q = \dot{m}\, C_p\, (\mathrm{T_{out}} - T_{in}) \qquad \text{(eq. 2)}$$

Then the instantaneous thermal efficiency of the collector can be calculated as shown in eq. 3.

$$\eta = \frac{\dot{m}\, C_p\, (\mathrm{T_{out}} - T_{in})}{A\, G} \qquad \text{(eq. 3)}$$

Where A is the collector area and G is the global irradiance on the collector (measured with the pyranometer). The measurements were made after waiting for the inlet temperature and mass flow rate to stabilise, then the values were recorded for at least 10 minutes at a rate of one measurement per second. Then the inlet temperature

was increased again and the process repeated. The efficiency was calculated for each sample and then averaged. To maximise ΔT, the temperature increase in the collector it was necessary to aim for as low mass flow rate as practical whilst maintaining flow in the turbulent regime.

3.5 Results – electrical output

The LSC cover was made up of four LSC modules with Sunpower solar PV cells along the two long edges. All the cells along the top of the LSC and all the cells along the bottom of the LSC are connected in parallel as shown in Fig. 11, these form two outputs at both the top and the bottom of the collector. The I-V curve measurements were taken with a laptop and Ketithley source measuring unit that were brought to the roof and connected to the LSC for measurement. Several measurements were taken, initially and after several hours of tracking. At least four measurements were taken at a time and averaged.

Fig. 12 left shows the I-V characteristics when the top row and bottom row were connected together in series. Fig. 12 right shows the P-V curves comparing top/bottom outputs connected in series (purple) and parallel (pink). The series connected output in pink has a maximum power of .220 W and performs better than the parallel connected output achieving only 0.167 W. With a power input on to the LSC area of 120 W gives an overall LSC cover efficiency of 0.183 %. This is an efficiency based on the AM 1.5 solar spectrum. The low power conversion efficiency can be explained by the low initial absorption of highly transparent pink Evonik sheet that initially only absorbs 8.6 % of the solar AM 1.5 spectrum, making this type of LSC suitable for generating modest amounts of power and transferring most of the solar energy to the thermal receiver.

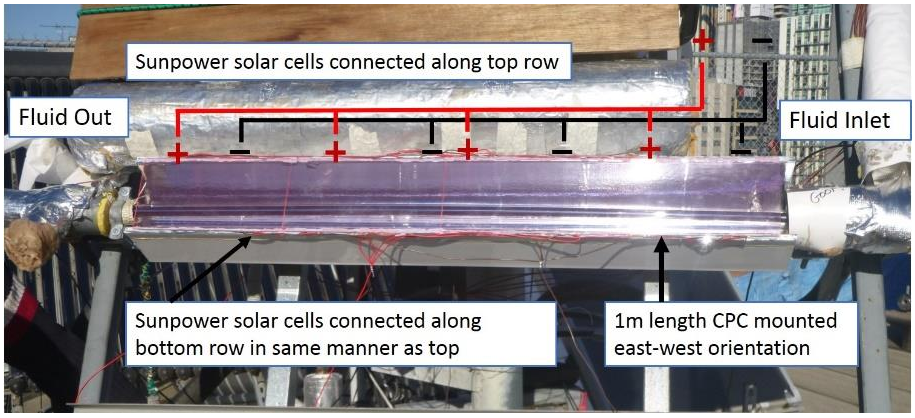

Fig. 2: LSC wiring for full length module

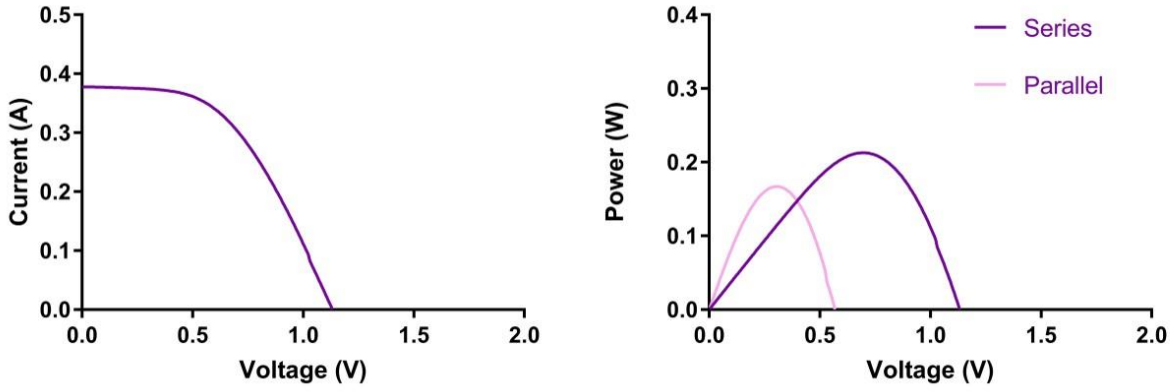

Fig. 12: I-V curve showing top and bottom output connected in series (left), P-V curve comparing top and bottom connected in series and in parallel (right)

3.5 Results – instantaneous thermal efficiency

The thermal performance of the collector was determined by obtaining values of instantaneous efficiency for combination of measured incident radiation, inlet/outlet temperatures and flow rate in a steady or quasi steady state. The useful power extracted is determined by eq. 3 and the thermal efficiency as a function of fluid inlet temperature is shown in Fig. 13. An uncertainty analysis was completed and the reason for the large error bars is due to the small ΔT across a single tube. While each RTD that measures inlet and outlet temperature has an uncertainty of +/- 0.082 ˚C when uncertainties are propagated due to taking a difference between the two measurements the uncertainty of ΔT becomes +/- 0.117 ˚C. Due to the high viscosity of the thermal fluid employed during the tests, a high flow rate had to be set in the experimental rig to assure turbulent flow and enhance heat transfer. This high flow rate decreases proportionally ΔT as shown in eq 2. In future work, a different heat transfer fluid which allows operating at lower flow rates or a longer receiver may be considered to increase the temperature at the outlet and minimise uncertainties in the measurements.

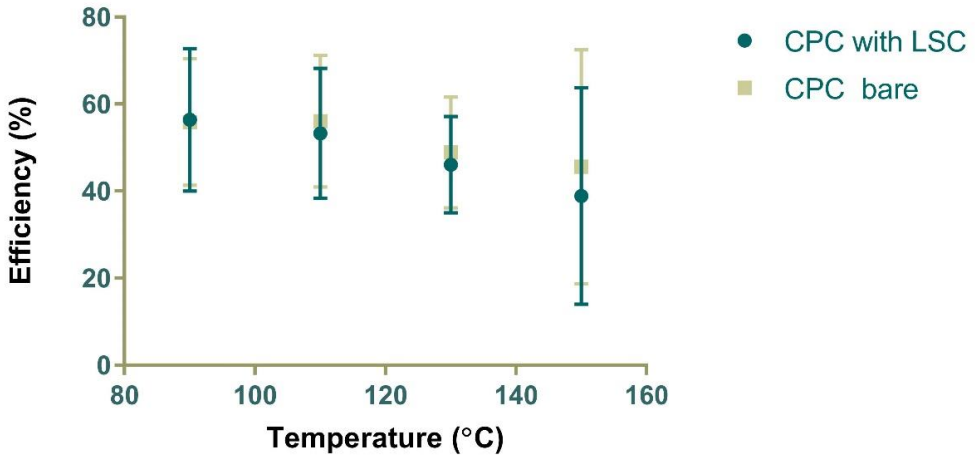

Fig. 3: Instantaneous thermal efficiency measured at different inlet temperatures

4. Conclusion

We successfully demonstrated the experimental basis for a new type of hybrid photovoltaic and thermal concentrator based on two non-imaging technologies, the CPC and the LSC. As a solar thermal collector requires a cover we have demonstrated a new type that generates electricity with LSCs. Utilising commercially available large area fluorescent sheets we demonstrated experimentally with a small prototype that a photovoltaic-thermal collector can work well when an LSC is used as a cover for a CPC. A small 10 cm x 15 cm prototype was stagnated in indoor test conditions and found to reach temperatures of up to 208 ˚C without an LSC and 191˚C with an LSC with a high transmission. In this configuration a small amount of thermal energy is sacrificed for a modest gain in electricity generation. Outdoor testing was completed on a full-length CPC and LSC hybrid collector with four LSC modules. It was found that less losses occurred (noticed by a much better fill factor) when the two sides of cells were connected in series, producing over 220 mW compared to parallel. I-V measurements were taken again after several hours of operation and it was found the performance of the LSCs did not decrease. This was most likely due to the experiment being run during cold days when ambient temperature was around 10-12 ˚C. The thermal efficiency was measured for a variety of temperatures and varied between 55 % and 40 % but with a high uncertainty. We demonstrated an LSC works well as a cover for a solar thermal receiver, although only generating modest amounts of power. The near future holds exciting possibilities of precisely engineering optical properties of LSCs. Perhaps one day we will be able to fabricate LSCs bottom up, molecule by molecule similar to 3D printing and once materials breakthroughs occur and LSCs can be engineering with tightly controlled optical properties, allowing for better performance of this type of PV-T collector.

5. References

Brunold, S., Frey, R., Frei, U., 1994. Comparison of three different collectors for process heat applications. SPIE 2255, Opt. Mater. Technol. Energy Effic. Sol. Energy Convers. XIII 2255, 107–118. doi:10.1117/12.185361

Carvalho, M.J., Collares-Pereira, M., Oliveira, J.C. De, Mendes, J.F., Haberle, A., Wittier, V., 1995. Optical and thermal testing of a new 1.2X CPC solar collector. Sol. Energy Mater. Sol. Cells 37, 175–190.

Debije, M.G., Verbunt, P.P.C., 2012. Thirty Years of Luminescent Solar Concentrator Research: Solar Energy for the Built Environment. Adv. Energy Mater. 2, 12–35. doi:10.1002/aenm.201100554

Evonik Industries [WWW Document], 2017. URL https://www.plexiglas-shop.cn/CN/en/category.htm?$category=9qlreq6bvlw (accessed 10.13.17).

Gajic, M., Lisi, F., Kirkwood, N., Smith, T.A., Mulvaney, P., Rosengarten, G., 2017. Circular luminescent solar concentrators. Sol. Energy 150, 30–37. doi:10.1016/j.solener.2017.04.034

Gallagher, J.. ., Winston, R., Duff, W.., 1993. Non imaging integrated evacuated solar collector. Int. Symp. Opt. Imaging, Instrum. 2016, 128–136.

Gu, X., Taylor, R.A., Morrison, G., Rosengarten, G., 2014. Theoretical analysis of a novel, portable, CPC-based solar thermal collector for methanol reforming. Appl. Energy 119, 467–475. doi:10.1016/j.apenergy.2014.01.033

Herrick, C.S., 1982. Optical transmittance measurements on a solar collector cover of cylindrical glass tubes. Sol. Energy 28, 5–11.

Hinterberger, H., 1966. Efficient Light Coupler for Threshold Cherenkov Counters. Rev. Sci. Instrum. 37, 1094. doi:10.1063/1.1720428

Kanellis, M., de Jong, M.M., Slooff, L., Debije, M.G., 2017. The solar noise barrier project: 1. Effect of incident light orientation on the performance of a large-scale luminescent solar concentrator noise barrier. Renew. Energy 103, 4–9. doi:10.1016/j.renene.2016.10.078

Karwa, N., Jiang, L., Winston, R., Rosengarten, G., 2015. Receiver shape optimization for maximizing medium temperature CPC collector efficiency. Sol. Energy 122, 529–546. doi:10.1016/j.solener.2015.08.039

Rabl, A., Winston, R., 1976. Ideal concentrators for finite sources and restricted exit angles. Appl. Opt. 15, 2880–3.

Rajkumar, V. a., Weijers, C., Debije, M.G., 2015. Distribution of absorbed heat in luminescent solar concentrator lightguides and effect on temperatures of mounted photovoltaic cells. Renew. Energy 80, 308–315. doi:10.1016/j.renene.2015.02.003

Ramos, A., Chatzopoulou, M.A., Guarracino, I., Freeman, J., Markides, C.N., 2017. Hybrid photovoltaic-thermal solar systems for combined heating, cooling and power provision in the urban environment. Energy Convers. Manag. doi:10.1016/j.enconman.2017.03.024

Slooff, L.H., Bende, E.E., Burgers, a. R., Budel, T., Pravettoni, M., Kenny, R.P., Dunlop, E.D., Büchtemann, A., 2008. A luminescent solar concentrator with 7.1% power conversion efficiency. Phys. status solidi - Rapid Res. Lett. 2, 257–259. doi:10.1002/pssr.200802186

Smestad, G., Ries, H., Winston, R., Yablonovitch, E., 1990. The thermodynamic limits of light concentrators. Sol. Energy Mater. 21, 99–111. doi:10.1016/0165-1633(90)90047-5

Winston, R., 1970. Light Collection within the Framework of Geometrical Optics. J. Opt. Soc. Am. 60, 245–247.

Winston, R., Wang, C., Zhang, W., 2009. Beating the optical Liouville theorem: How does geometrical optics know the second law of thermodynamics? Opt. Express 20, A622–A629. doi:10.1117/12.836029

Winston, R., Welford, W.T., 1978. Two-dimensional concentrators for inhomogeneous media. J. Opt. Soc. Am. 68, 289. doi:10.1364/JOSA.68.000289

Zhang, Z., Zhao, P., Lin, P., Sun, F., 2006. Thermo-optic coefficients of polymers for optical waveguide applications. Polymer (Guildf). 47, 4893–4896. doi:10.1016/j.polymer.2006.05.035